ISSN 0965-545X, Polymer Science, Ser. A, 2015, Vol. 57, No. 5, pp. 613–621. © Pleiades Publishing, Ltd., 2015.

Studies of Latex Blends of Natural Rubber/Poly(methyl methacrylate-*co*-2-ethylhexyl methacrylate) and their Comparison with Incompatible Natural Rubber/Poly(methyl methacrylate)[1]

Zhaojun Zheng, Xiaohui Tian, Jinyu Sun, Yizhong Yuan, and Bing Xie

School of Materials Science and Engineering, East China University of Science and Technology, Shanghai 200237, China

e-mail: tianxh@263.net

Received September 24, 2014;
Revised Manuscript Received April 23, 2015

Abstract—Poly(methyl methacrylate-*co*-2-ethylhexyl methacrylate) copolymers with 0.6–49.2 mol% of 2-ethylhexyl methacrylate were synthesized and blended with natural rubber at three different blend ratios (i.e. 5/95, 10/90, 15/85) on the latex stage. Chemical structure of the copolymer was confirmed by FTIR and ^{1}H NMR spectroscopy. Mechanical strength of the blend (rubber/copolymer) containing 7.76 mol% of 2-ethylhexyl methacrylate showed the higher values than the incompatible blend natural rubber/PMMA. According to water absorption and ATR-FTIR measurements, the amount of dispersed particles of obtained blends on the surface decreases sharply compared to rubber/PMMA blend. Scanning electron microscopy and atomic force microscopy also showed that surface and cross-section morphologies of the studied were more homogeneous than those of incompatible blend. The miscibility of studied blend was further reflected by DSC analysis.

DOI: 10.1134/S0965545X15050181

INTRODUCTION

Natural rubber (NR) latex, a well-known renewable material from Hevea brasiliensis, has been extensively utilized in the fabrication of dipped products, such as gloves, tubings, and dental dams for its good film-forming ability, tensile strength and resilience [1]. However, NR has a distinct drawback in anti-oxidation and heat resistance due to the presence of the carbon-carbon double bonds in the structure [2]. Besides, it is also urgent to reinforce the mechanical strength for further expanding the range of industrial application. Because of excellent weather resistance and mechanical strength of PMMA, the PMMA/NR blends have been attracting significant attention from academic and practical fields [3]. However, the blending is highly incompatible and immiscible due to the mismatch of the polarity and hydrophilicity [4].

There are two general methods to improve the compatibility between NR and PMMA. One of them is to prepare modified NRs from chemical reaction of NR and polar materials. The modified NRs mainly involve epoxidized natural rubber (ENR), maleated natural rubber (MNR) and graft copolymer of NR with poly(methyl methacrylate) (NR-*g*-PMMA) [5–7]. Nakason et al. [8] revealed that the morphology of ENR/PMMA blend steadily became smooth when the ENR content increased, and the glass transition temperature of NR phase gradually shifted to higher temperature with the increasing content of epoxide groups. These results showed the strong interactions between ENR and PMMA via the polar groups of each polymer. Nakason et al. [9] also studied the reactive compatibilization of MNR/PMMA blend in the molten state. From the analysis of morphologies it was found that the increase of MNR parts caused a decrease in the size of dispersed phase. In addition, Oommen et al. [10] reported the incorporation of NR-*g*-PMMA into the heterogeneous NR/PMMA blend as a compatibilizer. The NR-*g*-PMMA parts could effectively reduce the interfacial tension between the two different phases and improve physical properties of the immiscible blend. The other method is to synthesize the interpenetrating polymer network (IPN), which is a combination of two or more polymers in the network form [11]. Jayasuriya et al. [12] have studied an IPN composite obtained from the in situ polymerization of MMA in the NR films. It was clearly observed that tensile strength of the material was largely reinforced due to the massive formation of chemical interaction and crosslink between PMMA chains and NR chains.

Unlike the chemical interaction of polar materials, it is extremely convenient and inexpensive to improve the compatibility issue via the physical interaction. By blending NR with copolymer, the

[1] The article is published in the original.

Table 1. The composition of PMEMA copolymers

Sample	MMA, g	EHMA, g	EHMA, mol %	T_g, °C	Particle size, nm	$M_n \times 10^4$	M_w/M_n
PMMA	10	0	0	97.5	51.7	16	2.37
$PMEMA_1$	9	1	0.6	55.2	51.9	26	1.87
$PMEMA_2$	8	2	7.8	53.7	51.7	13	1.81
$PMEMA_3$	7	3	23.1	65.5	67.5	17	1.78
$PMEMA_4$	6	4	41.5	59.6	68.2	14	2.01
$PMEMA_5$	5	5	49.2	54.1	54.0	9	2.19

resulting material can exhibit more desirable properties [13–15]. For example, the blend of NR and poly(ethylene-*co*-vinyl acetate) (EVA) is reported to possess the good ageing resistance and mechanical strength [16]. Due to physical interaction between the non-polar units from EVA and non-polar NR chains, the interfacial tension between the two phases could be reduced [17–18]. In this work, we also prepared a series of copolymers with non-polar EHMA units. It was supposed that the non-polar interaction of the two components was beneficial for improving the interfacial adhesion at the boundary. Moreover, it is also well-known that a continuous and non-detective film from enormous interdiffsusion between the blend components is crucial to generate the necessary mechanical strength [19]. Besides, the polymer diffusion mostly occurs at temperature above glass transition temperature (T_g) of polymer [20]. Ho et al. [4] have reported the accumulation of incompatible PMMA particles on the film surface in the NR/PMMA latex blend. This is mainly due to the big differences in hydrophilicity and T_g (PMMA, $T_g >$ 100°C; NR, $T_g < -60$°C), the un-deformed and polar particles were easily trend to immigrate into the film surface through water channel during the film forming [21–22]. In this paper, a variety of poly(methyl methacrylate-*co*-2-ethylhexyl methacrylate) were synthesized. Due to the presence of EHMA units (PEHMA, $T_g = -10$°C), the T_g values of the copolymers were far less than that of PMMA. The results indicate that the diffusion of copolymers is stronger than that of PMMA at the film forming temperature (70°C). Thus, owing to the abundant interaction between PMEMA phase and NR phase, it was expected that the PMEMA copolymer could be compatible with NR.

EXPERIMENTAL

Material

NR latex (solid content: 60 wt %) was purchased from Hainan American International Xianghe Industrial (Hainan, China). 2,2-Azobisisobutyronitrile (AIBN, 98%) was provided by Shanghai Ling-Feng Chemical Reagent (Shanghai, China) and was recrystallized twice from ethyl alcohol before use. Tween 80 (Aldrich) and sodium dodecylbenzene sulfonate (SDBS, Aldrich) were used as surfactants. Methyl methacrylate (MMA, 99%, Aldrich) and 2-ethylhexylmethacrylate (EHMA, 99%, Aldrich) were purified by passing through a basic alumina column to remove inhibitor and distilled. Methanol and THF were from Aldrich (St. Louis, USA) and used without further purification. $CDCl_3$ for ^1H NMR analysis was obtained from Merck (Darmstadt, Germany). Deionized water was used throughout the experiment.

Preparation and Characterization of Polymers

The synthesis of polymers was performed in a four-necked, 150-mL flask with a mechanical stirrer, nitrogen inlet, a thermometer, and a condenser. Based on the purpose of simplicity, a series of PMEMA copolymers were subsequently coded as $PMEMA_1$, $PMEMA_2$, $PMEMA_3$, $PMEMA_4$, $PMEMA_5$ for the polymers with different EHMA/MMA mass ratios (g/g) of 1/9, 2/8, 3/7, 4/6, and 5/5, respectively (Table 1). In the preparation process, the mixture of MMA, EHMA, surfactants (Tween/SDBS = 1/1) and water was firstly added into the flask and stirred for 0.5 h at ambient temperature under high-purity nitrogen atmosphere. The reaction temperature was raised to 80°C, and the remaining mixture of monomers and initiator was then consecutively added into the reaction vessel over a 3 h period. The copolymerization was further conducted for 8 h followed by cooling down to room temperature. The resulting latex was sieved to remove any coagulum formed. The preparation of PMMA and PMEMA were similar. At the purification process, excessive methanol was poured into the polymer latex, followed by the precipitate was dissolved in THF, and then reprecipitated twice in methanol. The samples were finally obtained after being dried for 48 h in a vacuum oven at 70°C.

The purified sample was dissolved in THF and the resulting solution was then coated on KBr pellet for FTIR spectroscopy (Magna-IR550, Nicolet) measurement. To conduct ^{1}H NMR spectroscopy (AVANCE, Bruker), the polymer was dissolved into $CDCl_3$ at 25°C. The molar composition of EHMA in the PMEMA copolymer was determined by ^{1}H NMR spectroscopy and was calculated by Eq. (1):

$$M_{EHMA} = \frac{3B}{3B + 2A} \times 100\%, \quad (1)$$

M_{EHMA} is the molar percentage of EHMA in the copolymer, A and B are the area under the peaks designated as a and b, i.e. for $-OCH_3$ and $-OCH_2-$ protons, respectively.

A dried sample (5 mg) was put in an aluminum pan that was then hermetically sealed and run in the DSC instrument (DSC 2910, TA, US) from 25 to150°C at a heating rate of 20 deg/min.

The particle sizes of samples were obtained by Nano (ZEN3600, UK) at 25°C. The sample was diluted with distilled water to an appropriate concentration prior to the measurements. Twelve sub-runs were recorded for each measurement.

The number-average molecular weights and polydispersity indices of the polymers were determined by GPC at 25°C with PL-GPC50 using poly(methyl methacrylate) as a standard. *N*,*N*-dimethylformamide (DMF) was used as the eluent at a flowing rate of 0.8 mL/min, and the sample concentration was 2.0 mg/mL.

Preparation of NR/PMMA and NR/PMEMA Latex Blends and Their Characteristics

The preparation of latex blend involved two steps. In the first step, the pH value of polymer sample (PMMA or PMEMA) was adjusted to pH ≈ 10 by adding ammonia solution. In the second step, the blend of polymer latex and natural rubber latex was carried out by mixing different ratios (i.e. 5/95, 10/90, 15/85). The stirring was kept at ambient temperature using mechanical stirrers for 2 h in order to ensure a homogeneous, non-segregating blend. Film with a uniform thickness was prepared by pouring the blend into plastic culture dish and drying at 70°C for 12 h.

Mechanical strength tests were carried out according to GB 7543-2006 at room temperature. The specimens were prepared by cutting a film in a rectangular shape of 4 mm × 5 cm. Tensile strength and elongation at break of the samples were measured by universal test tension machine (CMT2202) at a rate of 400.0 mm/min. At least eight specimens were tested for each blend, and the average values were reported.

The accumulation of dispersed particles on the blended film surfaces was revealed by swelling measurement, ATR-IR (Magna-IR 550, Nicolet) spectroscopy. The 25 mm × 25 mm film specimen was weighed (W_0) and immersed in 10 ml of distilled water at room temperature for 24 h. After removal of residual water on the film surface, the hydrated film was reweighed (W_s), the swelling ratio was calculated by Eq. (2):

$$\text{Swelling ratio} = \frac{W_s - W_0}{W_0} \times 100\% \quad (2)$$

The micrographs of the blended film surfaces and cross-section images were examined by SEM (JSM-6360LV). Film samples were coated with gold in a sputter coater, their surface and cross-section morphologies (prepared under a liquid nitrogen atmosphere) were photographed at an appropriate magnification. The three-dimensional images of the blended films were analyzed by atomic force microscopy (AFM, Veeco/DI).

The glass transition temperatures of the blended films were examined by DSC. A film sample (5 mg) was placed in the hermetical aluminum pan and run in the DSC instrument (DSC 2910, TA, US) from −100 to 25°C at a heating rate of 20 deg/min under a liquid nitrogen atmosphere.

RESULTS AND DISCUSSION

Characterization of Chemical Structure of PMEMA

The chemical structure of PMEMA is presented below:

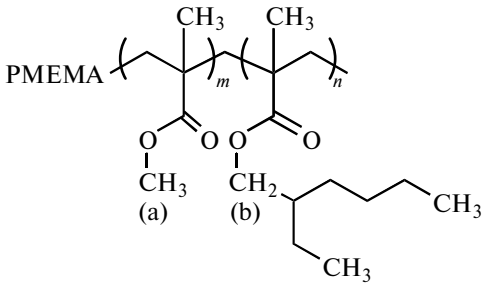

The characteristic bands, which may be referred to functional groups of MMA and EHMA units, are observed in the spectra of PMEMA (Fig. 1). Three bands at 1194, 1464 and 728 cm^{-1} may be assigned to C–O stretching of ester group in MMA units, the C–H scissoring vibrations of CH_2 and C–H rocking vibrations of CH_2 ($-(CH_2)_n$, $n \geq 4$) for EHMA units respectively [23–27]. Moreover, in the 3000–2800 cm^{-1}, another group of bands is observed, they can be assigned to C–H stretching of CH_3 (2995 cm^{-1})

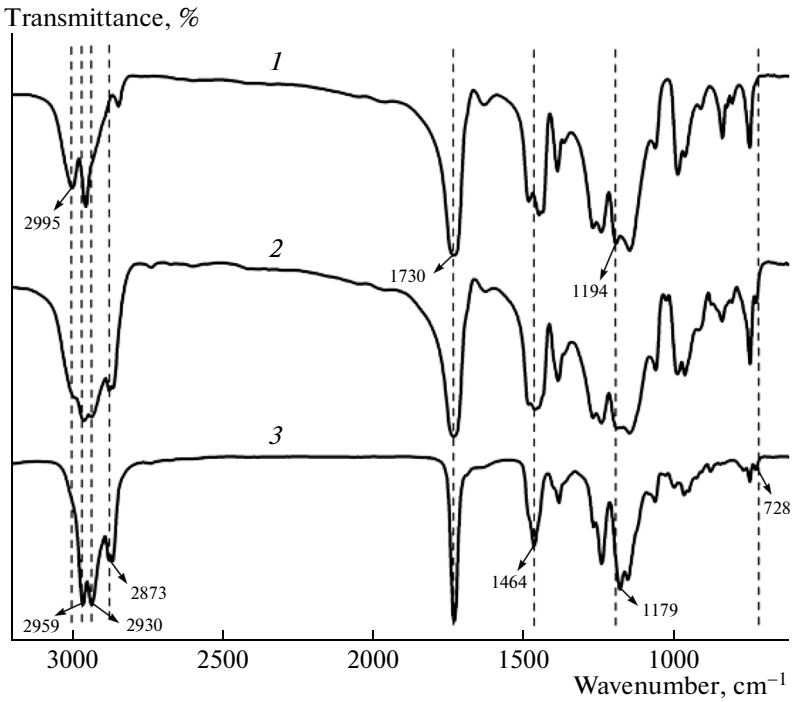

Fig. 1. FTIR of (*1*) PMMA, (*2*) PMEMA, and (*3*) PEHMA.

for MMA units and C–H asymmetrical stretching of CH_2 (2959 cm^{-1}), C–H stretching of CH_3 (2930 cm^{-1}), C–H symmetrical stretching of CH_2 (2873 cm^{-1}) for EHMA units [28–30].

According to the characterization data from FTIR, it is thus concluded that the copolymer prepared by EHMA monomer and MMA monomer is successfully synthesized.

Mechanical Properties

Tensile strength and elongation at break of NR/PMMA and NR/PMEMA blends are shown in Table 2, respectively. When PMMA is blended with rubbery materials, the PMMA material frequently acts a reinforcing agent to increase physical strength of the matrix and reduce its elasticity. Therefore, it is clearly found that the tensile strength of NR/PMMA and NR/PMEMA is higher than that of pure NR. However, it is interesting to note that the tensile strength of NR/$PMEMA_2$ blend is superior to the corresponding NR/PMMA blend. The highest tensile strength of NR/$PMEMA_2$ (90/10) (21.5 MPa) gives rise to a 10.3% increase compared to that of NR/PMMA(90/10) (19.5 MPa). This may be due to the sufficient interaction between PMEMA chains and NR chains, leading to the considerable entanglements of the two components and contributing to the reinforcement in physical strength. In addition, as shown in Fig. 4, elongation at break of NR/PMMA and NR/PMEMA blends both sharply decrease as the increasing concentration of PMMA or PMEMA, respectively. However, the elongation at break of NR/PMEMA blend is almost equivalent to the one of pure NR at the addition of 10 phr PMEMA with 49.18 mol% EHMA composition. Besides, it is also found that the descending trend of NR/PMEMA blends is gradually alleviated as the increasing percentage of EHMA units in the copolymer. This is mainly the fact that rubbery characteristic of EHMA units acts as a function of plasticizer to soften the blended films [31].

Characterization of Dispersed Particles on the Blended Film Surfaces

Water absorption of NR films containing different amounts of various polymers is also presented in Table 2. Because of non-polarity in the NR film, its water absorption is minimal in the experiment. Although the polarity of PMMA, the water absorption of NR/PMMA blend begins decrease beyond the addition of 10 phr. This is may be explained that the incompatible PMMA particles are considerably accumulated on the film surface, hindering the water molecules into the NR inner [4]. However, it is clearly noted that the water absorption values of modified films from copolymers are superior to that of modified films from homopolymer (PMMA). The result indicates that the amount of aggregating particles on the surface may be largely reduced. This is probably the

Table 2. Summary of mechanical properties for NR/PMMA and NR/PMEMA blends

Samples	Blend ratio (NR/PMMA or PMEMA)	Tensile strength, MPa	Elongation at break, %	Water absorption, %
NR	–	12.1 ± 0.1	1050 ± 40	95 ± 2
NR/PMMA	95/5	17.2 ± 0.3	920 ± 34	135 ± 2
	90/10	19.2 ± 0.4	830 ± 33	213 ± 3
	85/15	19.5 ± 0.4	700 ± 31	70 ± 2
NR/$PMEMA_1$	95/5	16.5 ± 0.3	930 ± 25	150 ± 2
	90/10	18.3 ± 0.4	850 ± 27	233 ± 3
	85/15	18.5 ± 0.4	730 ± 26	93 ± 2
NR/$PMEMA_2$	95/5	17.9 ± 0.4	950 ± 25	168 ± 2
	90/10	21.5 ± 0.5	870 ± 26	261 ± 3
	85/15	19.7 ± 0.4	820 ± 25	152 ± 2
NR/$PMEMA_3$	95/5	16.9 ± 0.3	970 ± 25	180 ± 2
	90/10	19.8 ± 0.4	900 ± 24	291 ± 3
	85/15	18.1 ± 0.4	850 ± 26	175 ± 2
NR/$PMEMA_4$	95/5	16.1 ± 0.3	1000 ± 26	160 ± 2
	90/10	17.9 ± 0.4	970 ± 25	250 ± 3
	85/15	17.2 ± 0.3	950 ± 25	133 ± 2
NR/$PMEMA_5$	95/5	15.5 ± 0.2	1010 ± 25	149 ± 2
	90/10	17.6 ± 0.3	980 ± 26	221 ± 3
	85/15	16.1 ± 0.3	960 ± 24	78 ± 2

reason that the compatibility of PMEMA/NR due to strong mobility and sectional non-polarity of PMEMA phase reduces the accumulation of dispersed particles. Additionally, it is also observed that the water absorption for NR/PMEMA blend initially reaches a maximum and then begins decrease, which is well consistent with the result of tensile strength. This is probably the reason that the presence of interfacial saturation from the sufficient interaction between the two phases, the excess of materials would be more inclined to migrate to the film surface and thus make water absorption reduced. Therefore, the improved properties of blended films could be obtained only with the addition of suitable amount of modified materials. Based on the above data, The 10 phr may be close to the optimum addition for enhanced properties.

The accumulation of dispersed particles on the blended film surfaces was further characterized by ATR-FTIR. As shown in Fig. 2, in the 1750–700 cm^{-1} region, the band at 1730 and 836 cm^{-1} are assigned to the C=O vibration from PMMA or PMEMA and C–H deformation vibration of cis C=C–H from NR, respectively. Among these blended films, it is clearly found that the intensity of NR/PMMA at 1730 cm^{-1} is a maximum, and the one at 836 cm^{-1} is a minimum. This is mainly the reason that the considerable aggregation of incompatible PMMA particles on the film surfaces. Three additional bands are also observed at 1448, 1375 and 1146 cm^{-1}, which are assigned to C–H deformation of $-CH_3$, C–H deformation of $-CH_2$ for NR and C–O–C stretching for PMEMA, respectively. Compared to the NR/PMMA blend, the intensities of NR/PMEMA blends at the 1448, 1375 cm^{-1} peak largely increase, and the one at the 1146 cm^{-1} adversely decrease. Besides, in the 3000–2800 cm^{-1} region of the infrared spectra, three bands are observed at 2957, 2914, 2851 cm^{-1} that are all assigned to C–H stretching of $-CH_3$ for NR. It is also found that the intensities of NR/PMEMA blends at the three peaks

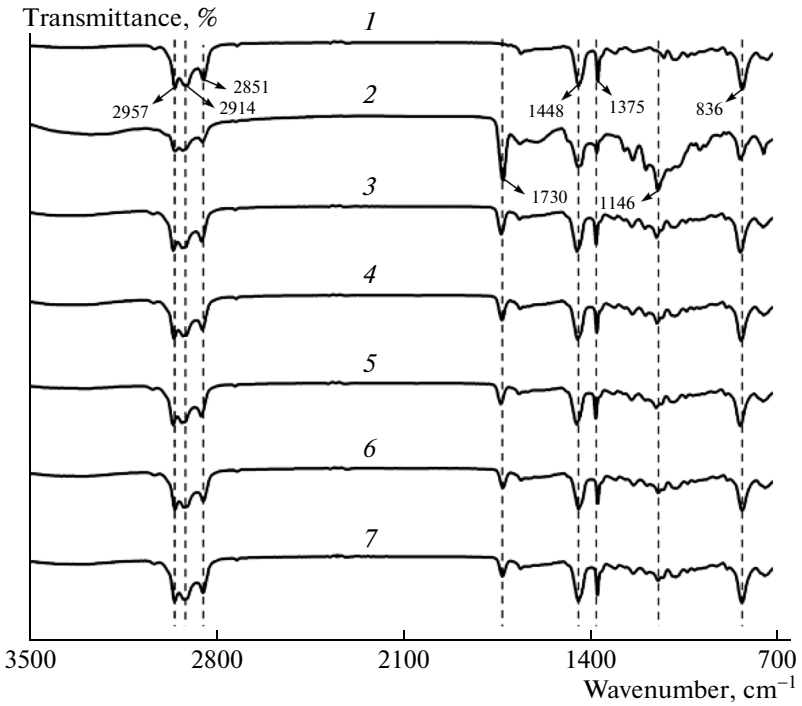

Fig. 2. ATR-FTIR of (*1*) NR, (*2*) NR/PMMA (90/10), (*3*) NR/PMEMA$_1$10 (90/10), (*4*) NR/PMEMA$_2$10 (90/10), (*5*) NR/PMEMA$_3$10 (90/10), (*6*) NR/PMEMA$_4$10 (90/10), and (*7*) NR/PMEMA$_5$10 (90/10) blends.

are stronger than the ones of NR/PMMA. These results clearly reveal that the amount of dispersed particles of NR/PMEMA blends remarkably decreases on the film surfaces, indicating the improvement in the compatibility of NR/PMEMA blends compared to that of NR/PMMA.

Morphologies

AFM is a powerful tool in the study of film morphologies because it could provide high resolution 3-D (3-dimensional) phase images of the film surfaces without destroying the samples. As shown in Fig. 3a, some round particles with the diameters varied from 400 to 1500 nm are randomly packing at the pure NR film due to the polydispersity of the NR particles, and thus the film surface is slightly uneven. Compared to pure NR film, the NR90/PMMA10 film surface was distributed numerous hills and deep cavitations (Fig. 3b). The hills may arise from the accumulation of hard PMMA particles during the film formation, and the cavitations are probably due to the massive aggregation of hard PMMA particle in the environment of soft rubber chains. As the incorporation of copolymers into the NR, it is clearly found that decreasing accumulation of dispersed particles on the surfaces (Figs. 3c, 3d) and their average roughness (Ra) values largely decrease. This result suggests that the high interfacial adhesion between NR phase and PMEMA phase, which can be beneficial for the formation of homogenous films.

The cross-section images of blended films are effectively and directly utilized to demonstrate the interfacial adhesion between the two phases. From Fig. 4a, it can be found that the cross-section morphology of NR film is smooth due to the mobility and homogeneity of soft rubber in the nature. Comparing to the images of NR, the fracture surface of NR/PMMA (90/10) (Fig. 4b) is heterogeneously distributed many cavities, suggesting a poor adhesion between the blend components. The cavities might be attributed to the slowly diffusion of the undeformed PMMA particles from the matrix films. However, the morphology of NR/PMEMA$_2$ (90/10) shows a dense film with less cracking and cavities (Fig. 4c). This result clearly confirms that the significant interaction between NR phase and PMEMA phase. In addition, as the increasing content of EHMA, it is also found a more smooth film with grey attachment from the deformation of soft EHMA units is obtained (Fig. 4d). From the above morphologies of blended films, it can be implied that the blend of NR/PMEMA is much more compatible than NR/PMMA blend.

DSC Characterization

To further confirm the compatibility between NR and PMEMA, differential scanning calorimeter

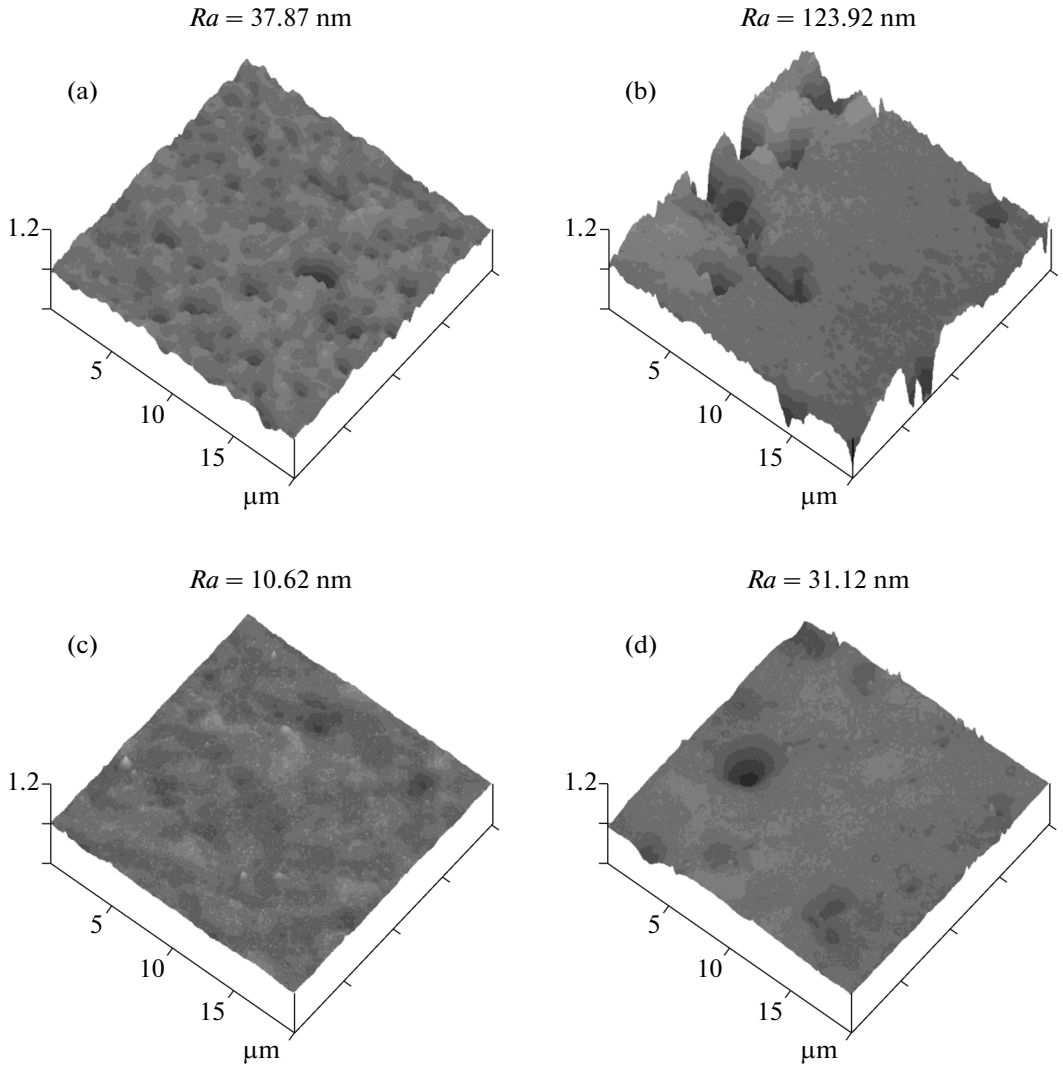

Fig. 3. AFM 3-D images of (a) NR, (b) NR/PMMA (90/10), (c) NR/$PMEMA_2$ (90/10), and (d) NR/$PMEMA_3$ (90/10).

(DSC) was used to analyze the glass transition temperatures of NR phase in the blends. As shown in Fig. 5, T_g values of NR phase of pure NR and NR/PMMA (90/10), NR/$PMEMA_2$ (90/10), and NR/$PMEMA_3$ (90/10) film are −63.0, −58.9, −58.6, −58.3°C, respectively. The gradually increasing T_g values indicates the enhanced interactions of copolymer chains and rubber chains, which can be considered as a improvement in interfacial adhesion between the blend components. Moreover, it is also noticed that the glass transition region of NR phase in the NR/$PMEMA_2$ blend is wider than that of NR/PMMA blend. This means that considerable formation of entanglements due to the stronger interdiffusion between the two components. Thus, these results suggest that the NR/PMEMA blend is more compatible than NR/PMMA.

CONCLUSIONS

A variety of copolymers were synthesized via free radical polymerization using a series of EHMA/MMA ratios and blended with NR in the latex. Based on the improved mobility and sectional non-polarity, these copolymers chains could effectively diffuse into rubber phase and contribute to the much enhanced entanglement between the two chains. Thus, the largely reinforcement in the tensile strength and sharply decrease in the amount of dispersed particles on the surface were clearly observed. From the surface and cross-section images of SEM and 3-D images of AFM, the highly homogeneous morphologies of NR/PMEMA blends indicated the strong interfacial adhesion between the blend components. Furthermore, the increasing T_g values of NR/PMEMA blends further confirmed the compatibility between the two phases. It was thus demonstrated that the copolymer was more

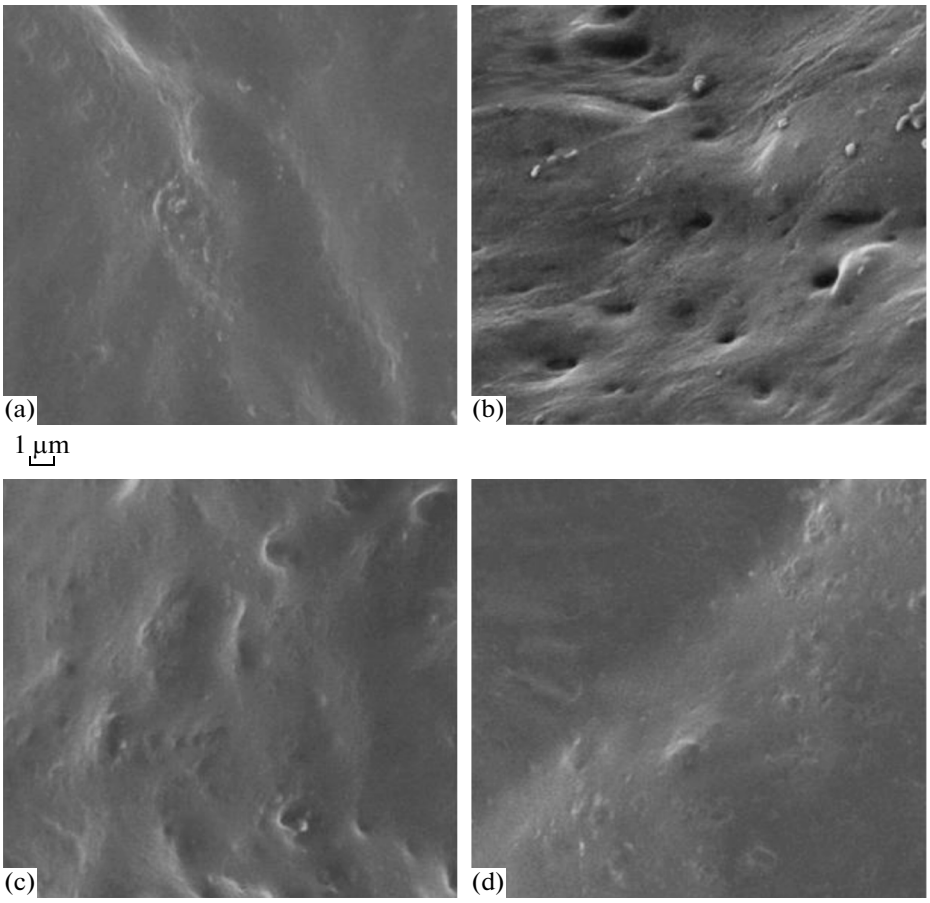

Fig. 4. SEM cross-section images of (a) NR, (b) NR/PMMA(90/10), (c) NR/$PMEMA_2$ (90/10), and (d) NR/$PMEMA_3$ (90/10).

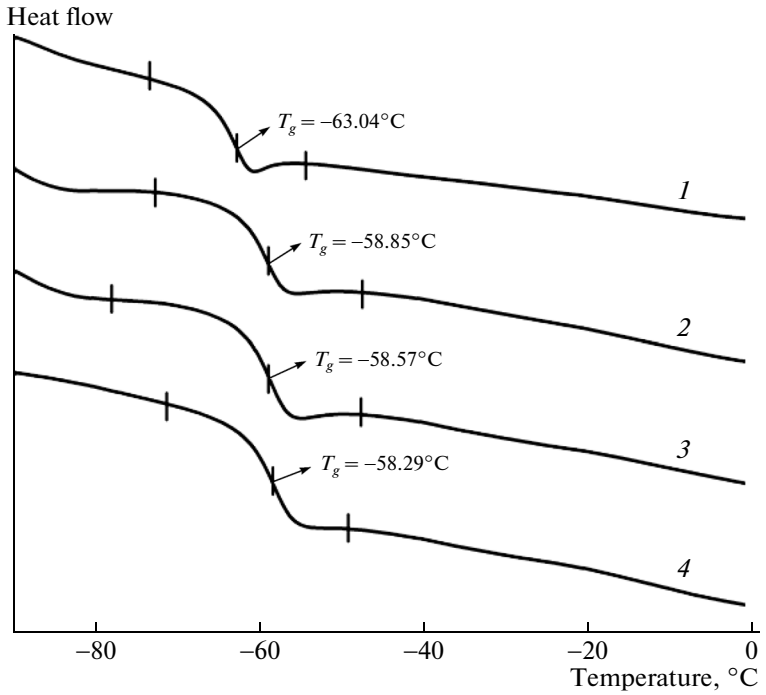

Fig. 5. DSC characterization of (*1*) NR, (*2*) NR/PMMA (90/10), (*3*) NR/$PMEMA_2$ (90/10), and (*4*) NR/$PMEMA_3$ (90/10).

compatible with NR than PMMA, and the composite films make the copolymers highly interesting for preparing dipped products with excellent tensile strength and elasticity.

ACKNOWLEDGMENTS

We thank for the financial support by National High Technology Research and Development Program (2009AA035002).

REFERENCES

1. M. M. Rippel, A. P. L. Carlos, and M. Fernando, Anal. Chem. **74**, 2541 (2002).
2. P. Piya-areetham, G. L. Rempel, and P. Prasassarakich, Polym. Degrad. Stabil. **102**, 112 (2014).
3. M. M. Jayasuriya and D. J. Hourston, J. Appl. Polym. Sci. **124**, 3558 (2012).
4. C. C. Ho, M. C. Knew, and Y. F. Liew, Surf. Interface. Anal. **32**, 133 (2001).
5. V. Tanrattanakul and T. Kaewprakob, J. Appl. Polym. Sci. **112**, 1817 (2009).
6. P. Wongthong, C. Nakason, Q. Pan, and G. L. Rempel. Eur. Polm. J. **49**, 4035 (2013).
7. C. Nakason, W. Pechurai, K. Sahakaro, and A. Kaesaman, J. Appl. Polym. Sci. **99**, 1600 (2006).
8. C. Nakason, Y. Panklieng, and A. Kaesaman, J. Appl. Polym. Sci. **92**, 3561 (2004).
9. C. Nakason, S. Saiwaree, S. Tatun, and A. Kaesaman, Polym. Test. **25**, 656 (2006).
10. Z. Oommen and S. Thomas, Polymer **38**, 5611 (1997).
11. L. H. Sperling, *Interpenetrating Polymer Networks and Related Materials* (Plenum, New York, 1981).
12. M. M. Jayasuriya and D. J. Hourston, J. Appl. Polym. Sci. **112**, 3217 (2009).
13. A. T. Koshy, B. Kuriakose, S. Thomas, and S. Varghese, Polymer **34**, 3428 (1993).
14. N. Hayeemasae, H. Ismail, and A. R. Azura, Polymplast. Technol. **52**, 501 (2013).
15. S. Chattopadhyay and S. Sivaram, Polym. Int. **50**, 67 (2001).
16. Z. Mohamad, H. Ismail, and R. C. Thevy, J. Appl. Polym. Sci. **99**, 1504 (2006).
17. P. Kumari, C. K. Radhakrishnan, S. George, and G. Unnikrishnan, J. Polym. Res. **15**, 97 (2008).
18. P. Jansen and B. G. Sores, Polym. Degrad. Stabil. **52**, 95 (1996).
19. J. R. Feng, M. A. Winnik, and A. Siemiarlzuk, J. Polym. Sci., Part B: Polym. Phys. **36**, 1115 (1998).
20. K. Jud, H. H. Kausch, and J. G. Williams, J. Mater. Sci. **16**, 204 (1981).
21. G. G. Cameron, D. Stewart, R. Buscall, and J. Nemcek, Polymer **35**, 3384 (1994).
22. C. C. Ho and M. C. Khew, Langmuir **16**, 2436 (2000).
23. L. Xie, X. Huang, C. Wu, and P. Jiang, J. Mater. Chem. **21**, 5897 (2011).
24. P. Bassan, H. J. Byrne, F. Bonnier, J. Lee, P. Dumas, and P. Gardner, Analyst. **134**, 1586 (2009).
25. S. Dirlikov and J. L. Koenig, Appl. Spectrosc. **33**, 555 (1979).
26. J. C. O. Villanova, E. Ayres, M. O. Reis, and R. L. Orefice, Polym. Bull. **68**, 931 (2012).
27. S. Shah, A. Pal, Rajiv Gude, and S. Devi, Eur. Polym. J. **46**, 958 (2010).
28. L. A. Cannon and R. A. Pethrick, Macromolecules **32**, 7617 (1999).
29. G. A. Wang, C. C. Wang, and C. Y. Chen, Polym. Degrad. Stabil. **91**, 2683 (2006).
30. S. Bajpai, J. S. P. Rai, and I. Nigam, J. Appl. Polym. Sci. **122**, 3152 (2011).
31. H. Eslami and S. Zhu, Macromol. Mater. Eng. **291**, 1104 (2006).